Component-specific Preliminary Engine Design Taking into Account Holistic Design Aspects

Marco Hendler, Michael Lockan, Dieter Bestle, Peter Flassig

Component-specific Preliminary Engine Design Taking into Account Holistic Design Aspects

Marco Hendler[1]*, Michael Lockan[1], Dieter Bestle[1], Peter Flassig[2]

ISROMAC 2017

International Symposium on Transport Phenomena and Dynamics of Rotating Machinery

Hawaii, Maui

December 16-21 2017

Abstract

Efficient aero engine operation requires not only optimized components like compressor, combustor and turbine, but also an optimal balance between these components. Therefore, a holistic coupled optimization of the whole engine involving all relevant components would be advisable. Due to its high complexity and wide variety of design parameters, however, such an approach is not feasible, which is why today's aero engine design process is typically split into different component specific optimization sub-processes. To guarantee the final functionality, components are coupled by fixed aerodynamic and thermodynamic interface parameters predefined by simplified performance calculations early in the design process and held constant for all further design steps. In order not to miss the optimization potential of variable interface parameters and the unlimited design space on higher-fidelity design levels, different coupling and optimization strategies are investigated and demonstrated for a reduced compressor-combustor test case problem by use of 1D and 2D aero design tools. The new holistic design approach enables an exchange of information between components on a higher-fidelity design level as well as the persecution of global engine design objectives like efficiency or emissions, and provides better results than separated component design with fixed interfaces.

Keywords

Holistic Optimization — Aero Engines — Aerodynamic Design

[1] *Department of Engineering Mechanics and Vehicle Dynamics, Brandenburg University of Technology, Cottbus, Germany*

[2] *Rolls-Royce Deutschland Ltd & Co KG, Blankenfelde, Germany*

*__Corresponding author__: hendler@b-tu.de

NOMENCLATURE

Symbols

DH	=	de Haller number
E_I	=	emission index
h	=	height
$\mathbf{h}$	=	constraint vector
l	=	length
m	=	mass
Ma	=	Mach number
p	=	static pressure, design variable
$\mathbf{p}$	=	design vector
P	=	feasible design space
r_{af}	=	air-to-fuel-ratio
s	=	mixing port style
T	=	temperature
x, r	=	axial/radial coordinate
$\boldsymbol{y}$	=	coupling vector
α	=	flow angle
γ	=	dimensionless port position factor
η	=	efficiency

Indices

$\bullet^{l,u}$	=	lower/upper bounds
$\bullet^{P}$	=	penalty values
$\bullet^{*}$	=	optimized values
$\bullet_{30}$	=	OGV outlet position
$\bullet_{B,C}$	=	combustor/compressor component
$\bullet_{i\|j}$	=	interface between two components
$\bullet_{HPC}$	=	bladed compressor section
$\bullet_{ex}$	=	outlet position
$\bullet_{h,t}$	=	hub/tip annulus line
$\bullet_{in}$	=	injector
$\bullet_{PD}$	=	pre-diffusor section
$\bullet_{pp,sp}$	=	primary/secondary mixing port
$\bullet_{pz,sz,dz}$	=	primary/secondary/delution zone
$\bullet_{SD}$	=	swan neck duct section

INTRODUCTION

Aero engine development is associated with both time and financial effort. To minimize development costs as well as risk, engine projects are often realized as divided processes in cooperation with other companies (joint venture) or as redesign based on established aero engines [1]. Advantageous for the division of tasks is the modular design strategy, where each component (fan, compressor, combustor and turbine) is designed independently from the others [2, 3]. The reason for such a component-based consideration is the high complexity in configuration and operation as well as the limited computational power available [4]. For the same reasons, aero engine design is split into different design phases with increasing degree of fidelity – starting with a simple and fast performance calculation up to a time-consuming 3D unsteady flow simulation [5, 6, 7]. To guarantee the final functionality after assembling all individually designed modules, interfaces between the components are pre-

determined. They are defined early in the multistage design process during the performance calculation based on thermodynamic models and remain constant in later higher-fidelity design phases.

Hence, a holistic analysis of the overall system is realized only in the very first design step. The subsequent, higher-fidelity autonomous design processes of the detailed design phase interpret these prescribed interfaces as fixed bounds and try to find their best results within these bounds. As the performance calculation does not consider geometric engine specifications, it may be expected that the interface state selection based on lower-fidelity performance models is not necessarily optimal, which finally leads to a non-optimal overall engine performance. Instead, the early definition of fixed interface states results in an unnecessary limitation of the design space for higher-fidelity and more precise design tools, which would be able to evaluate the affected interface states better and adapt them to find an overall optimal engine.

This raises the question as to how much potential is lost in current engine design projects by keeping the interface states fixed instead of allowing for modification by higher-fidelity tools during the design process. In the current paper an alternative design approach is presented where components of a two-shaft aero engine are designed together by using higher-fidelity design tools and variable interfaces. For simplification, the described test case is reduced to only two core engine modules: the high pressure compressor (C) and the combustor (B).

1. COMPRESSOR DESIGN PROCESS

The compressor module of a two-shaft aero engine consists of three main parts, Figure 1. The S-duct as first subcomponent (SD) transfers the incoming flow of the low pressure system (fan) to the faster rotating, high-pressure system moving on a lower radius. Downstream of the S-duct, the bladed annulus section (HPC) feeds power to the fluid for compression and the annulus cross section decreases substantially. Finally, the short diffusor section (PD) reduces the flow speed and directs the air mass flow into the combustion chamber.

The currently applied isolated compressor design procedure is based on a number of sub-processes with increasing degree of fidelity [5, 7] where interfaces to up- and downstream components are fixed and predefined based on a simplified thermodynamic performance calculation. For testing a large number of design configurations, only fast 1D and 2D design tools are used in the present research, whereas expensive 3D-CFD flow analysis may be executed at the end to receive detailed information about flow phenomena near the walls and about non-linearly conducted flow parameters.

To design the complete compressor section from S-duct inlet to diffusor outlet, a two-step approach is used here, where a 1D Meanline and a 2D Throughflow calculation are executed in combination. Objective of the compressor design sub-process is to search for a geometry configuration with best compressor efficiency η_C. In the first design step, the optimizer tries to find a valid compressor part from inlet guide vane (IGV) to outlet guide vane (OGV), i.e., in the HPC section, with the help of the 1D Meanline tool only. Therefore, different design parameters $\mathbf{p}_C$ concerning the shape of the annulus, stage pressure ratio, exit flow angles, and axial chord lengths are modified. The evaluation of the geometry takes place only at the midline part and ignores adjoining upstream and downstream compressor components, compare [5].

To receive more detailed information, a 2D streamline curvature analysis is executed for each valid Meanline compressor design. This analysis starts from the flow information of the former 1D calculation and is able to evaluate the complete compressor geometry including S-duct and diffusor. Here, flow information is determined in radial direction on different streamlines. The final information of the Throughflow calculation can then be used to generate aerofoils [8] and to build a 3D compressor geometry model for executing stress analyses or a multistage 3D-CFD.

Only with such an embedded compressor calculation taking the S-duct and diffusor into account, the relevant compressor interface values at the diffusor exit position can be determined properly and compared with the predefined values resulting from the performance calculation. Relevant interface parameters between compressor and downstream combustor component are exit flow angle α_{ex}, exit flow Mach number Ma_{30}, temperature T_{30} and pressure p_{30} as well as geometry

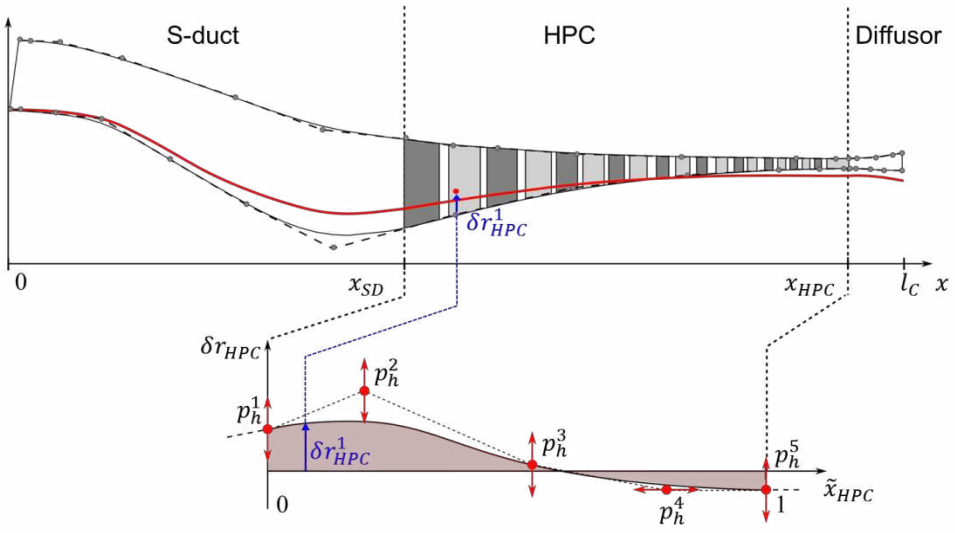

Figure 1. Compressor annulus parametrization strategy based on perturbation splines with an exemplarily shown modification of the hub contour

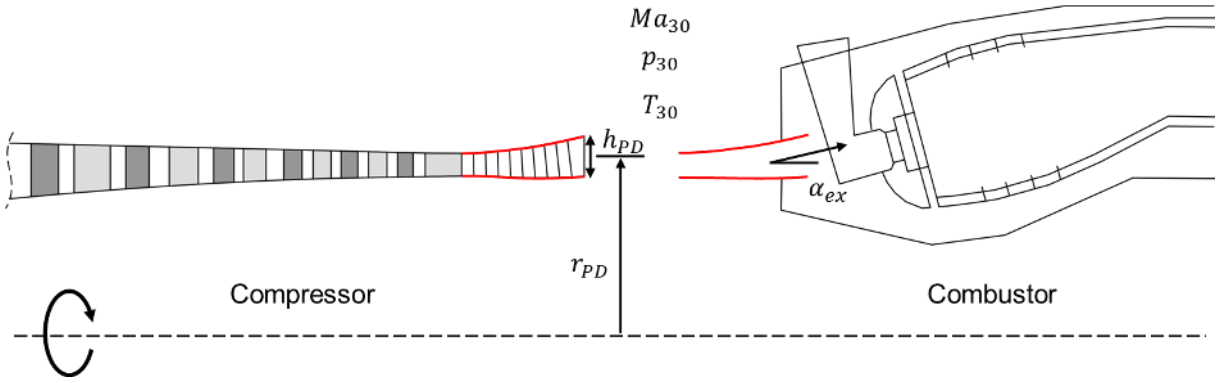

Figure 2. Geometric and aerodynamic compressor and combustor interface parameters

settings for mean radius r_{PD} and height h_{PD} of the diffusor exit plane, which are often set according to a reference engine. The aerodynamic and thermodynamic interface values, summarized in vector $\mathbf{y}_{C|B} = [\,\alpha_{ex}, Ma_{30}, T_{30}, p_{30}]^T \in \mathbb{R}^4$, are a result of the compressor flow analysis. Their compliance with the specifications of the performance calculation cannot be guaranteed in advance, but results during the optimization process. Therefore, they are considered as constraints which have to be fulfilled in order to obtain a feasible design. However, the geometric parameters $\mathbf{p}_{C|B} = [r_{PD}, h_{PD}]^T \in \mathbb{R}^2$ are adjusted at the beginning of the design process and held constant in state-of-the-art design strategies, Figure 2.

To ensure a valid compressor design, additional constraints limiting diffusion factors, de Haller numbers, stage works, inlet Mach numbers or surge margin according to [5] are considered as well. All these compressor specific constraints are summarized in $\mathbf{h}_C \leq \mathbf{0} \in \mathbb{R}^{36}$. This leads to the single objective compressor optimization problem

$$\max_{\mathbf{p}_C \in P_C} \eta_C$$
$$s.t.\;\; P_C = \{\mathbf{p}_C \in \mathbb{R}^{47} | \mathbf{h}_C(\mathbf{p}_C) \leq \mathbf{0},\; \mathbf{p}_C^l \leq \mathbf{p}_C \leq \mathbf{p}_C^u\} \tag{1}$$

with lower and upper bounds $\mathbf{p}_C^l$ and $\mathbf{p}_C^u$.

The biggest influence on finding a valid compressor geometry can be attributed to the design parameters of the inner and outer annulus contour which are represented by two B-spline curves and based on a reference compressor with a similar expectable contour. In a first design step, the reference contour lines are scaled to the actual inlet and outlet of the compressor and the scaled control points are then additionally modified within user-defined margins by the optimizer, see, e.g., lower annulus contour in Figure 1. To ensure the highest possible level of flexibility independent from the number of control points, their variation is controlled by separate perturbation splines for hub (h) and tip (t) with a lower, constant number of control points compared to the reference contour. An example for such an HPC hub section perturbation spline is given in the lower part of Figure 1. Thus, the control points of the reference annulus splines are not modified directly by the optimizer, but rather by the changes of the perturbation splines whose control points are actively modified. In order to reduce the dimension of the design space, perturbation information is only applied in radial direction by δr of the reference control points. Axial variations of the annulus control points would also be possible to allow for lengthwise modification of the compressor geometry. However, further perturbation mechanisms must be implemented and controlled, whereby the optimization effort increases as well as the run time to reach convergence.

Similar splines as in Figure 1 are given for all further parts of the contour lines, i.e., S-duct and diffusor. Each contour line is composed of three parts to allow for more individual design flexibility for each compressor part [9]. To guarantee an overall continuous perturbation spline, the transition control points to neighboring compressor parts are identical on both sides, respectively. Because of the fixed interface states in the current design strategy, the outer perturbation control points of the diffusor perturbation section are fixed to meet the predefined coordinates.

Special attention is payed to the properties of the diffusor part: it acts as adapter between compressor and combustor component with the task of converting dynamic pressure into static pressure and ensuring a low-loss inflow into the combustor section [10]. The exit flow of this component has significant influence on the flow of the combustor dome and on the air distribution inside the combustor. The large number of free contour variables in this section allows for the adjustment of different exit flow angles even for constant diffusor exit coordinates.

The presented parametrization strategy allows for the introduction of an additional design parameter which varies the influential length ratio between the bladed compressor part and the diffusor (l_{HPC}/l_{PD}), where the overall compressor length l_C is fixed as well as the swan neck duct length x_{SD}. This complicates the optimization effort on the one hand, but increases the design space on the other. The additional parameter may help to find a valid compressor design faster or to find more efficient design configurations. Some relevant geometric changes caused by perturbation of the design parameters are demonstrated in Figure 3, causing geometry modifications such as annulus outline, diffusor slope, length ratio, radial exit height or axial chord lengths.

The described compressor design process creates realistic flow results and provides a good basis for further 3D-CFD or mechanical stress analyses. Figure 4 displays a 2D flow field of an optimized compressor geometry. The absolute Mach number in the S-duct geometry is distributed homogenously with no local peaks, whereas the bladed section shows the desired intensive stressing of the hub profiles of the first rotor stations. The consideration of 36 specific constraints in $\mathbf{h}_C \leq \mathbf{0}$ ensures the aspired radially uniform outflow at the last high pressure compressor stator (OGV), a minimum annulus height for minimal flow blockage, and a diffusor geometry preventing flow separation. The last mentioned property is evaluated by a

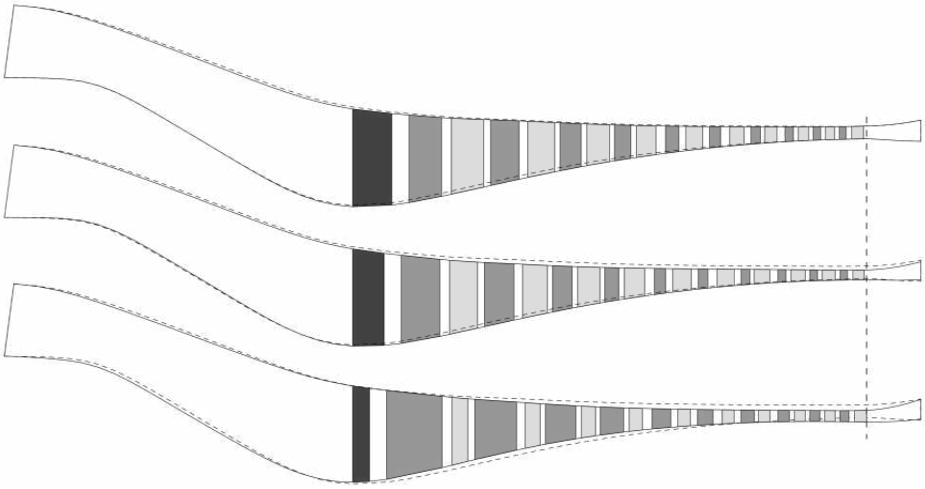

Figure 3. Possible annulus and aero block variations compared to a reference design (dashed line) by use of different design vectors $\mathbf{p}_C$ and fixed interface parameters $\mathbf{p}_{C|B}$

quality factor checking the inlet to outlet area ratio of the diffusor and comparing it to empirically determined limits.

2. COUPLING APPROACH

The isolated component design strategy presented above cannot guarantee to receive best overall engine performance, because the optimization potential lies in the modification of local design parameters only. To expand the design diversity and to find a globally optimal aero engine configuration, it is necessary to take into account the requirements of neighboring components. For the current test case, combustor design aspects are integrated into the compressor design process.

A simple process extension will not be sufficient because of the fixed interfaces given by the performance calculation or based on empirical values, which will force the design processes to one specific state. For example, if the compressor parameters are modified and the combustor module is only analyzed without changing its local design parameters, the result of the combustor will always be the same due to the unchanged interface. Therefore, interface values should be flexible and adaptable for higher-fidelity design processes, as this allows for a direct estimation of the compressor effects on the combustor module and finally on the overall design objectives.

Because of the significant influence of the interface parameters on the combustor performance, a parametrized combustor design process is needed which is able to recalculate the geometry and internal flow in every iteration loop. A fast state-of-the-art preliminary Rolls-Royce inhouse design tool is used which fulfills all necessary requirements regarding accuracy and flexibility. The tool uses internal design rules and correlations to provide all relevant aerodynamic flow parameters as well as a 2D combustor geometry, Figure 2. Key element of the tool is an internal flow solver adjusting the main geometric components within the given boundary conditions until, e.g., combustion stability, relight sizing, and desired Mach number distributions are fulfilled. Main objectives for the combustor design are to minimize the emissions and to maximize its efficiency η_B. The main emissions of carbon monoxide m_{CO}, nitrogen oxides m_{NO_x}, and unburned hydrocarbons m_{UHC} may be summarized in the emission index

$$E_I = \frac{m_{NO_x} + m_{CO} + m_{UHC}}{m_{Fuel}} \tag{2}$$

which equals the sum of the single emission values divided by the mass of injected fuel [11]. In order to influence the combustor outline and to optimize the efficiency and emission index, flow settings concerning the internal air distribution will be varied. Here, relevant design parameters are the air-to-fuel-ratios at injector $r_{af,in}$ and primary zone exit $r_{af,pz}$, length of primary and secondary combustion zones represented by the relative position of the related mixing ports (γ_{pp}, γ_{sp}), and the

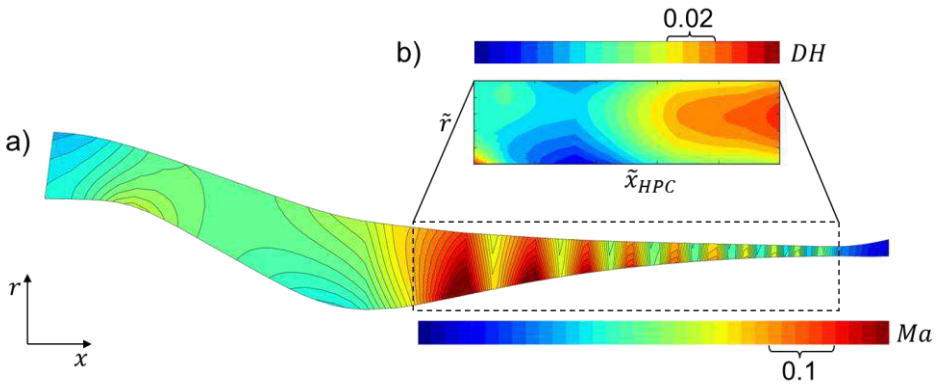

Figure 4. Axisymmetric meridional flow field of an optimized compressor geometry predicted by Throughflow: a) absolute Mach number contour plot $Ma = Ma(x, r)$ and b) de Haller criterion $DH = DH(\tilde{x}, \tilde{r})$ for the bladed part with respect to normalized axial and radial coordinates

style of the primary and secondary mixing ports (s_{pp}, s_{sp}) similar to [12]. The air-to-fuel ratios are related to the local mass flows at the injector as well as primary zone exit and are normalized by the fuel mass flow. They are the driving parameters for the inner combustor air distribution, Figure 5.

For a constant fuel mass flow, the air-to-fuel ratios affect the air flow distribution between mass flow passing the injector and the one flowing through the outer and inner annulus, see Figure 5. As already indicated, the position of the mixing ports is related to the length of the combustion zones. The length and volume of each combustion zone has a significant influence on the residence time of the air-fuel-mixture with a direct effect on the resulting emissions. For example, if the first mixing port is located further downstream, the hot primary zone is very distinctive and the residence time is high. This favors the relight ability, the fuel burn-out, and reduces CO generation. But for lower NO_x emissions it would be better to have only a small primary section and to leave the hot zone as quickly as possible. Hence, with the variation of the mixing port position the location can be defined where cooling air is fed and also what kind of emissions is generated.

The style of the mixing port defines the jet inclination angle and thus influences the jet penetration. Here two different port styles can be adjusted, which are represented by logical parameters s_{pp}, $s_{sp} \in \{0,1\}$. To get a plain mixing port style, which implicates a lower jet inclination angle, $s_\bullet = 0$ must be selected. In contrast, $s_\bullet = 1$ leads to a higher jet inclination angle. The final design vector results in

$$\mathbf{p}_B = \left[r_{af,in}, r_{af,pz}, \gamma_{pp}, \gamma_{sp}, s_{pp}, s_{sp}\right]^T. \tag{3}$$

Because of the high influence of the zonal combustor volumes on emissions and efficiency, they are taken into account by three inequality constraints $\mathbf{h}_B(\mathbf{p}_B) \leq \mathbf{0}$ during the design process based on internal design rules. The given constraints guarantee a combustor configuration which fulfills all ICAO admission requirements. Thus, the isolated compressor optimization problem reads as

$$\begin{aligned} \min_{\mathbf{p}_B \in P_B} & \begin{bmatrix} -\eta_B \\ E_I \end{bmatrix} \\ s.t.\ \ & P_B = \{\mathbf{p}_B \in \mathbb{R}^4 \times \mathbb{Z}^2 | \mathbf{h}_B(\mathbf{p}_B) \leq \mathbf{0}, \\ & \mathbf{p}_B^l \leq \mathbf{p}_B \leq \mathbf{p}_B^u, s_{pp} \in \{0,1\}, s_{sp} \in \{0,1\}\}. \end{aligned} \tag{4}$$

Due to the mixing port parameters in design vector $\mathbf{p}_B$, Eq. (4) is a mixed variable optimization problem. According to [5], this requires special strategies such as bound-and-cut algorithms by use of relaxation for example. A similar simple approach is used here as well. The optimizer works with continuous variables $\left[s_{pp}^*, s_{sp}^*\right]^T \in [0,1]^2 \subset \mathbb{R}^2$ instead of s_{pp} and s_{sp}. From these real values, mixing port styles are derived for analysis by

$$s_\bullet = \begin{cases} 0 \ for \ 0.0 \leq s_\bullet^* \leq 0.5 \\ 1 \ for \ 0.5 < s_\bullet^* \leq 1.0 \end{cases}. \tag{5}$$

3. HOLISTIC DESIGN STRATEGY

The consideration of several components in a coupled design process implicates a number of advantages, but specific challenges as well. For instance, impacts on downstream components by local geometry variation in upstream components can be evaluated directly and the findings gained can be applied in the following iteration loops. With regard to the present compressor-combustor test problem, not only the interface parameters $\mathbf{y}_{C|B}$ will be exchanged, but also the complete diffusor annulus geometry is handed over from the compressor to the combustor. The diffusor geometry is considered in both design processes because it is an integral part of both underlying design tools, i.e., the Throughflow solver of the compressor and the combustor design tool. Thus, the diffusor geometry is treated as an overlapping interface and exchanged to guarantee a consistent gas path geometry, otherwise the state-of-the-art compressor and combustor design processes would develop different diffusor interface sections independently from each other. The exchange of geometry information extends the design space and enables consideration of more design parameters like lengths modifications of the compressor subcomponents or unblocking of the radial interface coordinates by r_{PD} and h_{PD}. The last hub and tip control points of the compressor perturbation spline are now added as variables to $\mathbf{p}_c$ and the previously used parameters r_{PD} and h_{PD} in $\mathbf{p}_{C|B}$ at a specific transition point are replaced by the coordinates of the 2D hub and tip diffusor annulus contour. The transferred aerodynamic and geometric diffusor design information is used as input for the combustor component design process.

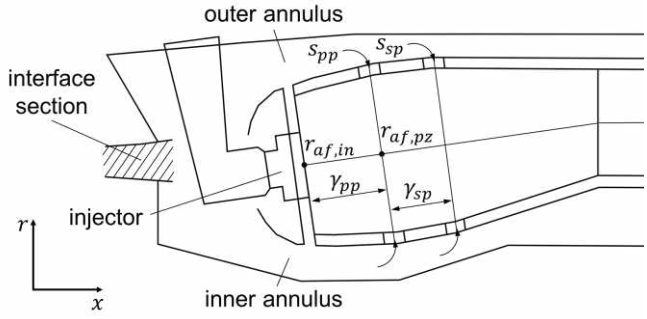

Figure 5. Combustor model with design parameters and overlapping interface area to the compressor

The geometry exchange between the two design processes impacts the performance prediction of both the compressor and the combustor. This would lead to a double-counting of the diffusor losses corrupting the overall efficiency. In order to avoid this corruption of an overall design criterion, the compressor efficiency value is read out directly behind the bladed part, i.e., at OGV exit, whereby the diffusor flow is not recognized in the compressor efficiency but still for the constraint calculation. However, through the extension the requirements and interests of different components must be combined. This leads to a multi-criterion optimization problem and a higher number of design parameters resulting in a more complex problem definition and design task.

Two different solution approaches for coupling the two engine components will be investigated. The first design approach is an all-at-once strategy, where both component design processes are integrated into a single optimization process and all design parameters are managed simultaneously by the overall optimizer, Figure 6a. The sub-processes are executed sequentially, where the upstream compressor component is executed first and determines the input parameters $\mathbf{y}_{C|B}$ and $\mathbf{p}_{C|B}$ for the subsequent combustor component. Due to prediction limitations of the involved design tools, upstream coupling effects from the combustor onto the compressor such

as the pressure increase in the combustor dump region are neglected here. If the design process is extended by higher fidelity design tools, upstream flow information should be considered and evaluated as well. After execution of both processes the results are returned to the optimizer. The global design problem formulation combines Eqs. (1) and (4) and represents a multi-criterion optimization problem [13] with design parameters $\mathbf{p} = [\mathbf{p}_C^T, \mathbf{p}_B^T]^T$ and constraint functions $\mathbf{h} = [\mathbf{h}_C^T, \mathbf{h}_B^T]^T$. However, to reduce the number of global objectives, the efficiency values are multiplied to receive the whole engine efficiency $\eta = \eta_C \eta_B$. This leads to the bi-criterion optimization problem

$$\begin{aligned} &\min_{\mathbf{p}\in P} \begin{bmatrix} -\eta_C\eta_B \\ E_I \end{bmatrix} \\ &s.t. \quad P = \left\{ \mathbf{p} = \begin{bmatrix} \mathbf{p}_C \\ \mathbf{p}_B \end{bmatrix} \in \mathbb{R}^{54} \times \mathbb{Z}^2 \middle| \mathbf{h} = \begin{bmatrix} \mathbf{h}_C \\ \mathbf{h}_B \end{bmatrix} \leq \mathbf{0}, \right. \\ &\qquad \left. \mathbf{y}_{C|B}^l \leq \mathbf{y}_{C|B} \leq \mathbf{y}_{C|B}^u, \mathbf{p}^l \leq \mathbf{p} \leq \mathbf{p}^u \right\}. \end{aligned} \tag{6}$$

Lower and upper bounds for the interface quantities $\mathbf{y}_{C|B}$ are determined to ensure feasible designs with regard to empirical knowledge.

In order to reduce the number of design variables in the overall optimizer, a second design process is proposed with a separated combustor optimization, Figure 6b. In contrast to the all-at-once approach, the global optimizer concentrates on the compressor optimization and varies the compressor design variables only. The combustor design process is not executed for every converged compressor optimization. Only if a compressor configuration fulfills all compressor constraints $\mathbf{h}_C \leq \mathbf{0}$ and lies within the interface bounds $\mathbf{y}_{C|B}^{l,u}$, a subsequent combustor optimization is performed. The combustor optimization searches for an optimal combustor geometry for the given set of interface parameters $\mathbf{y}_{C|B}$ and $\mathbf{p}_{C|B}$ by varying $\mathbf{p}_B$.

To reduce the computational time of the combustor optimization according to problem (4), only a single-criterion optimization is executed. Since the combustor efficiency for the considered "cruise" flight cycle is very high and almost invariant, it is not considered as an objective anymore, but as a constraint with a lower bound. All in all, this leads to the modified optimization problem

$$\begin{aligned} &\min_{\mathbf{p}_B\in P_B^*} E_I(\mathbf{p}_B, \mathbf{y}_{C|B}, \mathbf{p}_{C|B}) \\ &s.t. \quad P_B^* = \left\{ \mathbf{p}_B \in \mathbb{R}^4 \times \mathbb{Z}^2 \middle| \mathbf{h}_B(\mathbf{p}_B, \mathbf{y}_{C|B}, \mathbf{p}_{C|B}) \leq \mathbf{0}, \right. \\ &\qquad \left. \mathbf{p}_B^l \leq \mathbf{p}_B \leq \mathbf{p}_B^u, \eta_B^l \leq \eta_B(\mathbf{p}_B, \mathbf{y}_{C|B}, \mathbf{p}_{C|B}) \right\}. \end{aligned} \tag{7}$$

However, the higher-level optimizer will receive both values, i.e., the optimal emission $E_I^* = \min E_I$ and the associated combustor efficiency η_B^*, to calculate the overall efficiency and to evaluate the overall engine performance as in the all-at-once approach. If no valid compressor design exists for a given set of parameters, penalty values $E_I = E_I^P$ and $\eta_B = \eta_B^P$ for the combustor objectives as well as the design variables are handed over to the higher level optimizer to indicate a corrupt design. While hard coded extreme values are used for the objectives, penalty values are added to the minimum or maximum constraints for the design variables to emphasize the exceeding of the constraint boundaries. In summary, system design problem

$$\begin{aligned} &\min_{\mathbf{p}_C\in P_C^*} \begin{bmatrix} -\eta_C\eta_B^* \\ E_I^* \end{bmatrix} \\ &s.t. \quad P_C^* = \left\{ \mathbf{p}_C \in \mathbb{R}^{50} \middle| \begin{bmatrix} \mathbf{h}_C \\ \mathbf{h}_B \end{bmatrix} \leq \mathbf{0}, \right. \\ &\qquad \left. \mathbf{y}_{C|B}^l \leq \mathbf{y}_{C|B} \leq \mathbf{y}_{C|B}^u, \mathbf{p}_C^l \leq \mathbf{p}_C \leq \mathbf{p}_C^u \right\} \end{aligned} \tag{8}$$

needs to be solved for the decoupled optimization approach.

4. RESULTS

To demonstrate the benefits of a holistic compressor-combustor design process and to investigate differences between the two proposed coupling strategies, two optimizations have been performed. Starting point of the investigations is the reference design $\mathcal{R}$. It has been obtained by geometric scaling and aerodynamic cloning of an existing, approved design to given geometric and aerodynamic boundary conditions. Subsequently, it has been optimized separately with regard to the design problems in Eq. (1) and Eq. (7) with fixed interface values.

In contrast to the optimization of the reference design $\mathcal{R}$, the interface parameters $\mathbf{y}_{C|B}$ and $\mathbf{p}_{C|B}$ are not fixed during the holistic design process, but kept variable within defined ranges. This leads to an increased design space and offers completely new possibilities in the configuration and design of the individual components as well as the interface section. The larger the range of the variables, the higher is the degree of variation.

To solve the all-at-once problem in Figure 6a, an optimization for the design problem (6) is performed by using the Archive-based Micro Genetic Algorithm (AMGA) [14]. In total, 10000 design evaluations with a maximum population size of 40 have been evaluated, see Table 1. For the decoupled compressor-combustor design problem the AMGA is used with similar settings to optimize the system performance according to

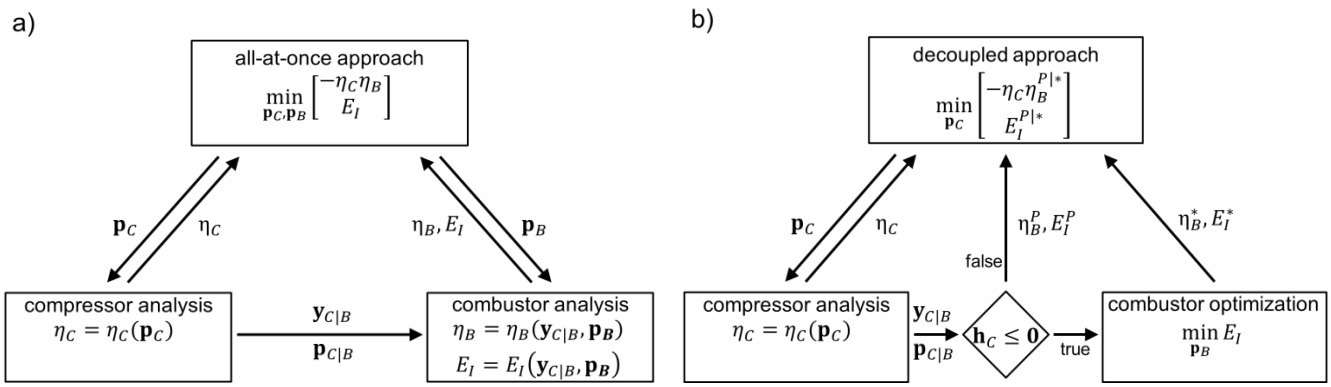

Figure 6. Investigated holistic design concepts: a) all-at-once-approach and b) decoupled combustor optimization

Eq. (8). In addition to this, the single objective optimization algorithm Covariance Matrix Adaptation Evolution Strategy (CMA-ES) [15] is executed to optimize the decoupled combustor, see Figure 6b, with regard to design problem (7). The number of function evaluations for each CMA-ES search, which is executed only for valid compressor configurations, is set to 160 or 20 generations with a population size of 8 only. With these settings sufficient convergence accuracy can be obtained with the help of the used tools.

Table 1. AMGA optimizer settings

optimizer settings	value
initial population size	500
population size	40
function evaluations	10000
archive size limit	1000
Pareto size limit	100

In direct comparison of compressor and combustor design processes, the combustor analysis takes 20 times longer than the used compressor design evaluation. To reduce this execution time discrepancy for utilizing both design strategies in an efficient manner and to make them more attractive for industrial application, the time intensive combustor performance prediction is replaced by a response surface. A radial basis function model is used to emulate effects of relevant combustor parameters. The data volume of the surrogate model is based on an initial Latin hypercube sampling [16] with 300 design evaluations which are generated before execution of the optimization. The use of a surrogate model leads to a significant reduction of the combustor design tool response time by a factor of 400, see Table 2. Further, the differences in computational time between both strategies become equalized and the total optimization time is reduced.

As can be seen in Figure 7, the holistic optimization yields non-dominated solutions (represented by black triangles and circles), which are better in both criteria compared to the reference design $\mathcal{R}$. Also, differences between the all-at-once approach and the decoupled strategy are visible: Although shown results may change for another search because of the random nature of evolutionary algorithms, it is interesting that the all-at-once optimization was able to identify discontinuities in the Pareto-front. The discontinued shape, in particular for the emission index, is due to the binary character of the chuting port style parameters s_{pp} and s_{sp}. If the first mixing port style, i.e., for the primary zone, is set to plain and the secondary to chuted, lowest emissions are obtained. Compared to this, the two optimal configurations of the all-at-once optimization with high emissions do have chuted port styles. Reasons why the decoupled strategy converged into the feasible design space with plain mixing ports only are: (i) low number of function evaluations for each individual combustor optimization and (ii) an early convergence of the top level optimization since combustor optimizations are only executed for feasible compressor designs. The results of Figure 7 have been confirmed in several runs, whereby the obtained representations of the Pareto-fronts are not exactly identical due to the utilization of evolutionary optimization algorithms. Further investigations are required to gain more confidence.

From an automated search perspective, an all-at-once approach is always the preferable option because only one optimization needs to be performed and convergence into local minima or local sets of non-dominated solutions is less likely. Additionally, the process architecture is clear and thus more user friendly. On the other side, an all-at-once strategy includes the most design parameters, here 56. A high number of design variables makes the optimizer inefficient, e.g., it takes longer to initialize the initial design space and the increased number of possible parameter conditions complicates the achievement of convergence. Furthermore, the coupled sequential design strategy with an immediate combustor analysis for each converged but not necessarily valid compressor design configuration increases the calculation time as well.

In contrast, the separated combustor optimization design strategy has the potential to obtain a valid engine design within a shorter period of time after starting the process. At first, the fast 1D and 2D compressor design tools are able to optimize the compressor geometry without disturbance until a valid design is obtained. The combustor optimization is then performed only for valid designs in order to find a matching combustor geometry fulfilling all design rules. With further design evaluations the compressor design process will propose more and more valid designs. For each of these designs a complete combustor subsystem optimization with 160 function evaluations is performed. From that point on the overall computational time would substantially increase without the use

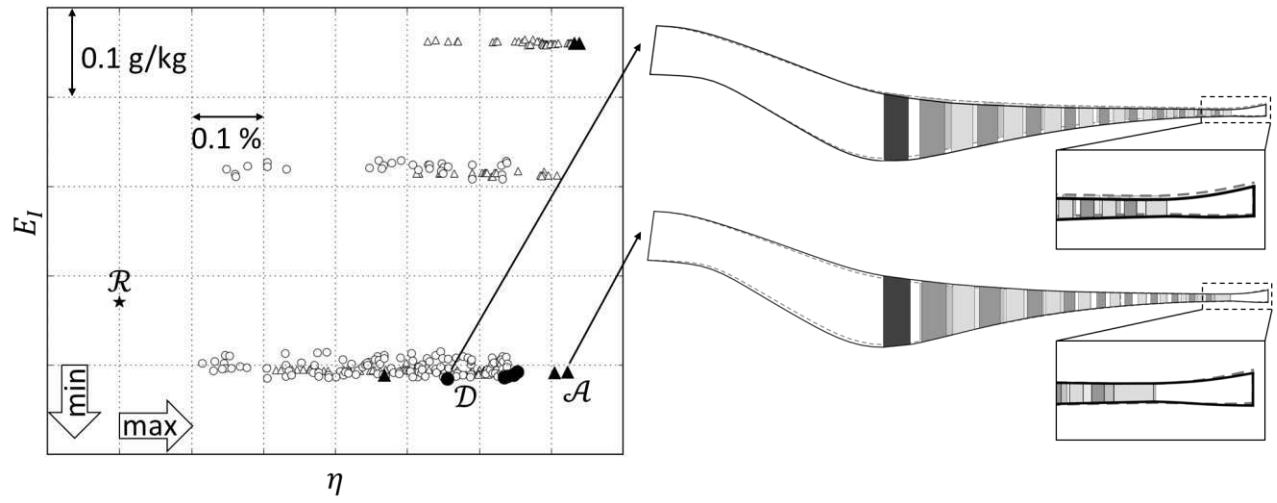

Figure 7. Visualization of feasible optimization results in the bi-criterion space with reference design ($\mathcal{R}$), all-at-once optimization results (triangles) and decoupled compressor-combustor optimization results (circles)

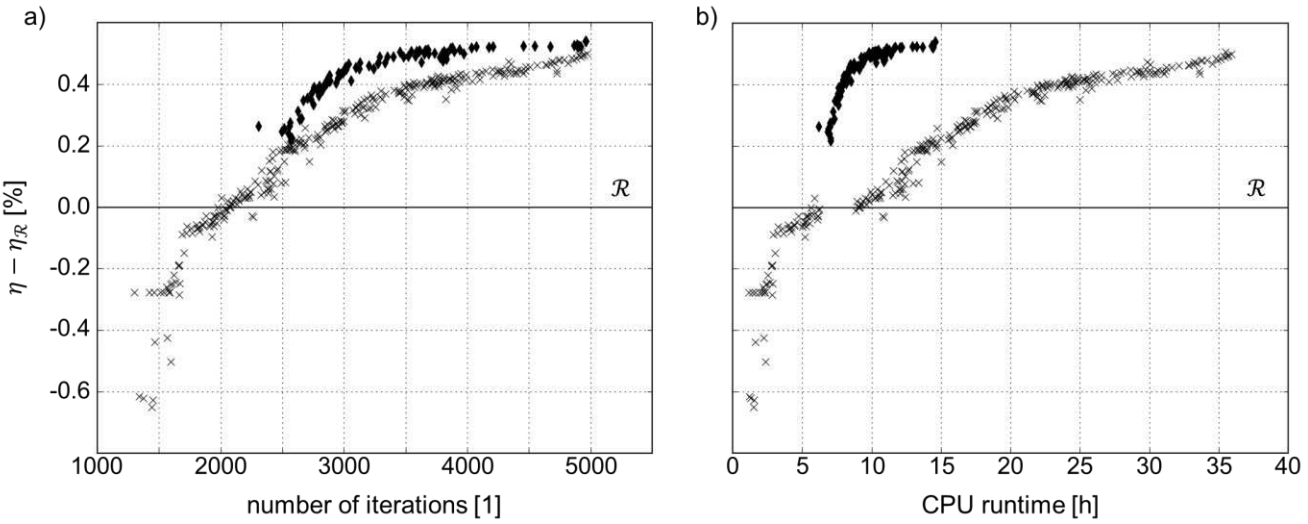

Figure 8. Representative convergence behavior of all-at-once optimization (diamonds) and decoupled optimization (crosses) in comparison to reference design ($\mathcal{R}$) for first 5000 runs for a) efficiency against number of iterations and b) efficiency against CPU time

of a surrogate model.

Figure 8 representatively shows the behavior of both design strategies for the first 5000 iteration steps while searching for an optimal solution for the problems (6) and (8). The efficiency objective is plotted against the number of iterations, Figure 8a, and the CPU time, Figure 8b. It is clearly visible that the decoupled optimization strategy (crosses) is able to find a first valid design four to five times faster than the all-at-once approach (diamonds) due to the reasons named above. Especially the consideration of a higher number of constraints as well as the execution of both the compressor and the combustor design tool for every single iteration lead to a less efficient convergence of the all-at-once approach at the beginning of the design process. The extended runtime in this phase, however, enables the optimizer to find a more efficient first valid design compared to the decoupled approach. With regard to the overall runtime, the all-at-once approach is up to three times faster for the same number of iteration steps because of the single combustor performance analysis for each compressor design proposal instead of executing a complete subsystem optimization. As can also be seen in Figure 8, with the decoupled approach a higher number of valid designs is identified, see Table 2, although the first designs are underperforming in comparison to $\mathcal{R}$, while all valid designs of the all-at-once approach are instantly more efficient than $\mathcal{R}$. Nonetheless, the final best efficiency values are nearly the same for both processes.

In summary, the selection of the design strategy depends on the intentions or requirements of the user: If an optimal design has to be found within a restricted time frame, the all-at-once approach should be applied. However, if a target value must be met as quickly as possible, the decoupled strategy would be the preferred option. Nevertheless, direct consideration of all component-specific design trends in every design step of the all-at-once approach allows an early consideration of individual design requirements and the creation of a widely dispersed holistic engine population. This finally leads to slightly better results when comparing both methods, see Figure 7. The main settings and time requirements of both optimization strategies are summarized in Table 2.

Both all-at-once and decoupled strategy may be seen as suitable here. In case of Intellectual Property Rights (IPR) problems and component specific separation of the development departments, an all-at-once approach with full software access is not feasible and the decoupled approach is preferred, where sharing of local design parameters and constraints (here $\mathbf{p}_B$ and $\mathbf{h}_B$) as well as specific parametrization strategies is not required. The combustor design process of the decoupled approach is similar to a black box, only the interface parameters are shared and the result is fed back to the overall design process.

Table 2. Process settings and runtimes

	all-at-once strategy	**decoupled strategy**
number of design variables (global/local)	56/0	50/6
number of objectives (global/local)	2/0	2/1
number of constraints (global/local)	40/0	37/3
runtime compressor eval.	~ 10.0 sec	~ 10.0 sec
runtime combustor eval. (with/without surrogate model)	~ 0.5 sec/ ~ 200.0 sec	~ 80.0 sec/ ~ 9.0 h
overall runtime	14.5 h	35.9 h
number of valid designs	95	295
first valid design found (iterations/time)	2037/6.2 h	1298/1.1 h

However, it must be kept in mind that the decoupled strategy is an optimization double-loop. Fully converged, i.e., optimal combustor designs cannot be guaranteed, because noisy combustor results are fed back to the global search. This is due to the fact, that the evolutionary optimization algorithm CMA-ES is used for the individual combustor search according to Eq. (7). Future studies with an increased number of design evaluations to investigate the level of uncertainties are conducted at the moment. Nonetheless, in comparison to $\mathcal{R}$, better results are obtained, independently of the choice of the holistic design approach.

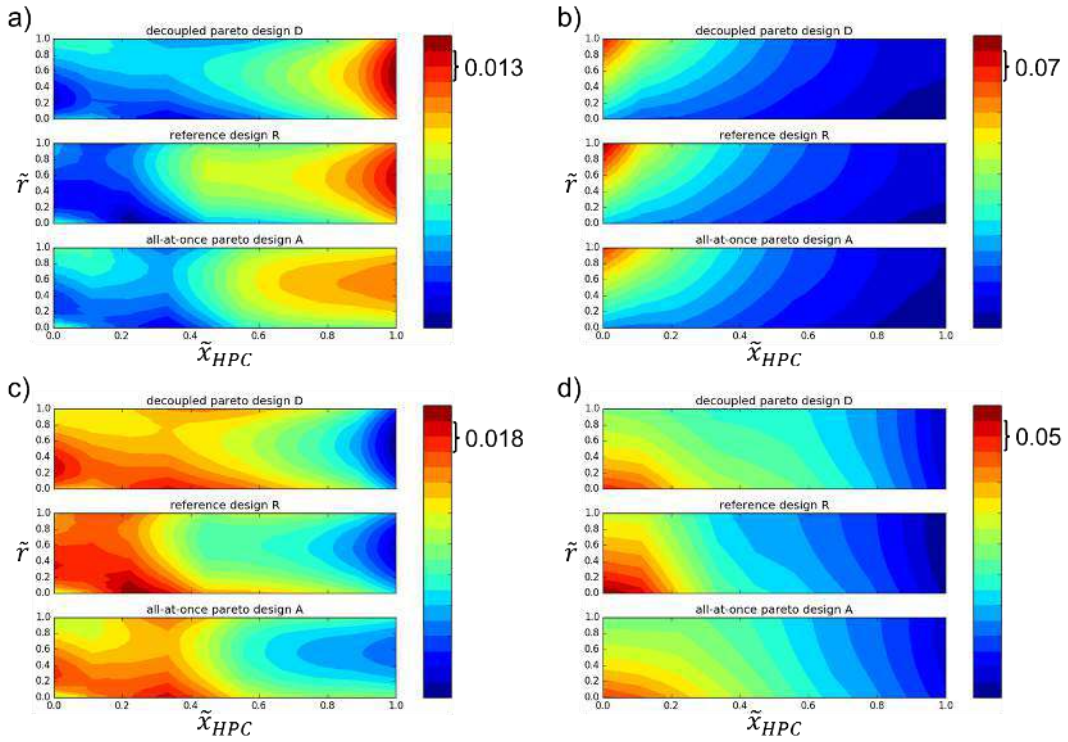

Figure 9. Optimization results of designs $\mathcal{A}$ and $\mathcal{D}$ compared to reference design $\mathcal{R}$: a) rotor de Haller number, b) rotor relative inlet Mach number, c) rotor static pressure rise and d) stator inlet Mach number

In Figure 7, annulus geometries for design $\mathcal{A}$, representing a non-dominated solution with low emissions from the all-at-once strategy, and design $\mathcal{D}$, corresponding to designs with minimal emissions from the decoupled approach, are shown and compared to the reference design $\mathcal{R}$. For all three configurations ($\mathcal{R}$, $\mathcal{A}$, $\mathcal{D}$) similar overall design requirements, e.g., compressor overall pressure ratio, shaft speed, environment conditions, etc., have been used. As can be seen, the annulus outline for both designs $\mathcal{A}$ and $\mathcal{D}$ deviates from the reference design $\mathcal{R}$. While the cross section area of design $\mathcal{A}$ increases especially in the S-duct section and the first stages of the bladed part, the annulus contour of design $\mathcal{D}$ is located on a lower mean radius with similar cross section areas.

The performance benefits can be explained by the geometry adaption and the consequently changed aerodynamic flow conditions. For both compressor configurations $\mathcal{A}$ and $\mathcal{D}$ the inflow to the bladed part was optimized. Figure 9b and 9d show a more homogeneous velocity profile in radial direction at the first rotor and stator positions. Additionally, lower relative tip Mach numbers, especially at inlet of rotor one and two, and decreased inlet Mach numbers at the front stator compared to the reference geometry are clearly recognizable. The lower velocity results in a decreased loading in the front part of the compressor, which is indicated by lower de Haller numbers and lower stage pressure ratios shown in Figure 9a and 9c. This leads to lower flow loss around the blades and, thus, higher efficiency. The loading decrease of design $\mathcal{A}$ compared to $\mathcal{R}$ is higher than the reduction between $\mathcal{D}$ and $\mathcal{R}$. This can be traced back to the increased cross section area for the same mass flow rate.

Furthermore, the axial chord lengths as well as the space-to-chord ratios have been changed. The increased space-to-chord ratios for design $\mathcal{A}$ and $\mathcal{D}$ lead to a reduced number of blades which results also in lower losses because of less wall interactions and finally in an increased efficiency. However, the geometric changes may result in a minor reduction of the surge margin, which is still acceptable and uncritical as the surge margin constraint needs to be fulfilled anyhow.

Several interface values initially set to the fixed interface parameters of design $\mathcal{R}$ have changed during the holistic optimization. Compared to the reference design, the temperature T_{30} was reduced by six degrees in design $\mathcal{A}$ and $\mathcal{D}$ with a constant overall compressor pressure ratio. This finally leads to a higher cooling performance of the air flow in the combustion chamber supporting the cool down of the hot combustion gas and stopping the NO_x production. Moreover, the materials are not loaded so heavily.

The diffusor geometry has changed towards a lower diffusor exit height, a lower exit mean radius and a longer compressor bladed part in configuration $\mathcal{D}$, where the latter leads to a shorter diffusor part. Design $\mathcal{A}$ has a diffusor exit geometry similar to $\mathcal{R}$, but a shorter bladed part resulting in a longer diffusor and lower exit flow angle.

The present geometry changes have to be discussed in the context of mass distribution as it is an important criterion for overall engine design. This step has been neglected in the present paper because of the focus on aerodynamic gas path design. The release of the interface parameters supports the design flexibility as it is now possible to meet a range of parameters rather than having to meet specific values which are often based on experience or defined too early in the design process by limited tools.

5. CONCLUSION

The present paper examines two different design approaches in order to develop complex aero engines more efficiently from

a holistic point of view and takes a coupled compressor and combustor system into account with the help of suitable parametrization and optimization strategies. For this purpose, state-of-the-art design methods and guidelines with fixed interfaces between the engine components are discarded and replaced by extended design processes, which allow for an exchange of information between neighboring components to enable the optimization of global rather than local design objectives. This is achieved by the variation of the annulus geometry and the aero blocks of the bladed compressor part as well as the extension of the design space by flexible aerodynamic and geometric interface parameters. Both the presented all-at-once approach and the compressor optimization process with a decoupled combustor optimization show better results compared to a reference design with isolated consideration of components regarding efficiency and emission index. The flexible interfaces and the extended design space also enhance a better convergence behavior.

Current design strategies allow only for downstream information transfer; in future work other coupling methods must be examined with regard to upstream information transfer as well [17]. Furthermore, compressor configurations shall not be determined only by combustor criteria, but also by other components as turbine or fan in order to make more precise statements about optimal compressor properties. Additionally to the component specific process, fidelity may be increased by the use of 3D analyzing tools to receive a multi-fidelity holistic approach as it was already done for the stand-alone compressor design process in [5].

ACKNOWLEDGMENTS

This work has been carried out in collaboration with Rolls-Royce Deutschland as part of the research project VITIV (Virtual Turbomachinery with Integrative Strategies, Proj.-No. 80164702) funded by the State of Brandenburg, the European Regional Development Fund, and Rolls-Royce Deutschland. Rolls-Royce Deutschland's permission to publish this work is greatly acknowledged.

REFERENCES

[1] J. M. Stricker and C. M. Norden. Computerized Preliminary Design of Turbomachinery. ASME Turbo Expo, Orlando, 91-GT-391, 1991.

[2] W. J. G. Bräunling. Flugzeugtriebwerke: Grundlagen, Aero-Thermodynamik, ideale und reale Kreisprozesse, Thermische Turbomaschinen, Komponenten, Emissionen und Systeme. Springer, Berlin, 2009.

[3] R. Parchem, P. Flassig and H. Wenzel. Collaborative Robust Engine Design Optimization. SIMULIA Community Conference, Vienna, 2013.

[4] S. Kim, J. Schlüter, X. Wu, J. J. Alonso and H. Pitsch. Integrated Simulations for Multi-Component Analysis of Gas Turbines: RANS Boundary Conditions. AIAA Conference, Fort Lauderdale, AIAA-2004-3415, 2004.

[5] F. Pöhlmann. Optimization and Coupling Strategies for Codes of Different Fidelity to Automate an Aerodynamic Compressor Design Process. Dissertation BTU Cottbus, Shaker, Aachen, 2015.

[6] M. Hinz. Neue Parametrisierungsstrategien und Methoden der Prozessbeschleunigung für die Verdichteroptimierung. Dissertation BTU Cottbus, Shaker, Aachen, 2012.

[7] T. Rühle. Ein Beitrag zur optimalen, mehrkriteriellen Axialverdichterauslegung auf Basis der Meridianströmungsrechnung. Dissertation BTU Cottbus, Shaker, Aachen, 2013.

[8] A. Dutta. An Automated Multi-Objective Optimization Approach for Aerodynamic 3D Compressor Blade Design. Dissertation BTU Cottbus, Shaker, Aachen, 2011.

[9] M. Hendler, S. Extra, M. Lockan, D. Bestle and P. Flassig. Compressor Design in the Context of Holistic Aero Engine Design. AIAA Aviation Forum, Denver, AIAA-2017-3334, 2017.

[10] V. R. Sanal Kumar, A. Muraleedharan, Y. Khan, A. Arokkiaswamy and R. M. O. Gemson. Studies on Dump Diffusers for Modern Aircraft Engines. AIAA Aviation Forum, Cincinnati, AIAA-2007-5161, 2007.

[11] ICAO Airport Air Quality Manual. URL: http://www.icao.int/environmentalprotection/Documents/Publications/FINAL.Doc%209889.1st%20Edition.alltext.en.pdf, accessed 12.04.2017.

[12] A. Angersbach and D. Bestle. Optimization of Air Distribution in a Preliminary Design Stage of an Aero-Engine Combustor. AIAA Aviation Forum, Atlanta, AIAA-2014-3004, 2014.

[13] D. Bestle. Analyse und Optimierung von Mehrkörpersystemen. Berlin, Springer, 1994.

[14] S. Tiwarir, P. Koch, G. Fadel and K. Deb. AMGA: An Archive-based Micro Genetic Algorithm for Multi-objective Optimization. GECCO'08, Atlanta, 729-736, 2008.

[15] N. Hansen. The CMA Evolution Strategy: A Comparing Review. StudFuzz 192, 75-102, 2006.

[16] W. L. Loh. On Latin hypercube sampling. Annals of Statistics, 33(6): 2058-2080, 2005.

[17] M. Lockan, D. Bestle, C. Janke and M. Meyer. Optimization of Coupled System Components Using Approximations of Interface Quantities. ASME Turbo Expo, Charlotte, GT2017-64135, 2017.